Novel Method Based Upon Combined Lidar System for PM2.5 Detection

Meng Li, Ning Fu, Xinglong Xiong, and Yuzhao Ma

***Abstract*—In this paper, we proposed a novel method based upon Lidar, atmospheric transmissometer and particle size spectrometer for PM2.5 detection. Combining the transmissive visibility meter and a particle size spectrometer, we can establish the relationship between PM2.5 mass concentration and atmospheric transmittance in vertical space. Then, with the transmissive visibility meter and Lidar, the vertical distribution of the atmospheric transmittance detected by the Lidar can be corrected. Compared with the direct use of particle size spectrometer and Lidar to retrieve the PM2.5 mass concentration profile, our method not only can determine Lidar boundary value effectively, but also settle the issue of incomplete overlap zone between the transmitter and the receiver to a certain extent. With real data, the proposed method is verified.**

***Index Terms*—Lidar, atmospheric transmissometer, particle size spectrometer, PM2.5 detection.**

I. Introduction

ATMOSPHERIC aerosol, or particular matter, refers to a stable multiphase system composed of solid and liquid particles suspended in the atmosphere [1], and directly affects the materialized state and radiation balance of the atmosphere by interacting with solar radiation [2], [3]. As the primary pollutant in the atmosphere, PM2.5 is the atmospheric aerosol with diameters less than 2.5 μm, which has adverse effects on human health [4], because the 24-h averaged PM2.5 concentration must be less than 65.5 $\mu g/m^3$ for healthy conditions [5], [6]. In addition, the extinction effect of PM2.5 on visible light is the main factor resulting in low atmospheric visibility and leading to the urban atmospheric haze [7], which seriously impact the safety of the flight and ground transportation [8]. Therefore, researchers domestic and abroad carried out extensive research on the PM2.5 detection and its the vertical distribution characteristics [9], [10].

For measuring the vertical distribution of aerosol extinction coefficient or other aerosol properties, several tools are designed and proposed, involving balloon, aircraft detection, as well as remote sensing [11]–[15]. Measurement instruments can be deployed on aircrafts or balloon to detect the PM2.5 distribution vertically [11]. However, taking the expensive costs of both manpower and resources into account, the measurement of remote sensing is the most effective method to detect the vertical profiles of PM2.5 on a continuous basis [12]. As a sophisticated instrument of remote sensing, Lidar is commonly employed to measure the vertical profiles of PM2.5 due to its high temporal-spatial resolution, wide detection range, and high detection accuracy [13]–[15]. Li [16] applied the Raman Lidar to retrieve aerosols, which can automatically avoid the atmospheric layers with the presence of aerosols, clouds and low signal to noise ratio (SNR). Zhang [17] used the Lidar system to detect the aerosol backscattering coefficient, relative humidity of the atmosphere at the same time and place, and retrieve the profile of PM2.5. Tao [18] detected the vertical distribution of extinction coefficient in Hefei based on the backward scatter Lidar, then calculated the PM2.5 mass concentration profile. Nevertheless, for the standard monostatic Lidar system, there is a large uncertainty in the selection of the boundary value of the Lidar in the upper air, which will potentially impact the calibration of the boundary value of the Lidar, and the accuracy of the PM2.5 mass concentration profile. Meanwhile, due to the geometric structure of monostatic Lidar system, there is an incomplete overlap zone between the transmitter and the receiver, the properties of PM2.5 cannot be characterized accurately [19]–[21]. Therefore, some novel combination instruments in terms of Lidar system are proposed, such as the CCD camera based Lidar, and Lidar Network, *et al.* In 1993, Meki first developed a imaging Lidar system involving a CCD camera and a Lidar for qualitative atmospheric measurements [22]. Then, Barnes employed wide-angle optics instead of a scanning system to design a CCD-camera based Lidar system for covering a larger altitude range. After that, several detection instruments based on similar techniques were proposed to measure the vertical distribution of PM2.5 and its optical properties [23], [24]. This kind of techniques capture the backscattering signals of laser on imaging principle, which can avoid the incomplete overlap zone effectively. But for the boundary value of the Lidar, it is still difficult to be selected.

Pertaining to the technique of Lidar Network, Welton [25]–[27] proposed a novel ground based eye-safe Lidar network, termed as Micro-Pulse Lidar Network (MPLNET), which can be used to acquire long- term observations of PM2.5 vertical profiles at unique geographic site. Based upon the Aerosol Robotic Network (AERONET) sun photometer and a Micro-Pulse Lidar Network (MPLNET) instrument, Chew [28], [29] investigated the relationships between ground-, satellite- and model-based aerosol optical depth (AOD) and PM2.5 for air quality assessment. Undoubtedly, Lidar network is an effective tool to measure

Manuscript received October 25, 2021; accepted November 16, 2021. Date of publication November 18, 2021; date of current version December 8, 2021. This work was supported in part by National Key R&D Program of China under Grants 2020YFB1600103 and 2020YFB1600101. *(Corresponding author: Ning Fu.)*

The authors are with the Key Laboratory of Operation Programming & Safety Technology of Air Traffic Management, Civil Aviation University of China, Tianjin 300300, China (e-mail: 867750570@163.com; lm867750570@163.com; 1078350688@qq.com; 13682022241@139.com).

Digital Object Identifier 10.1109/JPHOT.2021.3129190

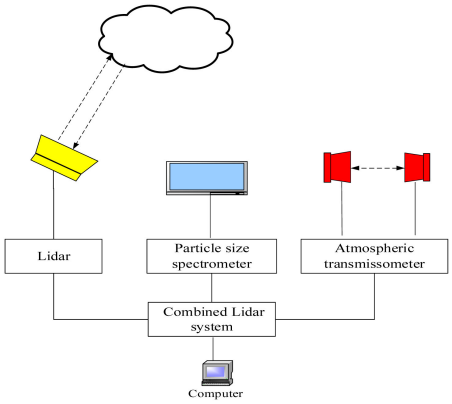

Fig. 1. Structure of detecting system.

TABLE I
KEY PARAMETERS OF LIDAR

Parameter	Value
Wavelength	1064 nm
Pulse energy	550 mJ
Pulse repetition rate	50 Hz
Scanning range	360°×90°
Telescope diameter	300 mm
Etalon bandwidth	170 MHz
Detector quantum coefficient	18%
Resolving distance	15 m
Maximum detection range	5 km

the vertical distribution of PM2.5 and its properties accurately, but the expensive cost of the Network construction hinders the application and development of this technology.

In this paper, we proposed a novel combined Lidar system that involves a Lidar, an atmospheric transmissometer as well as a particle size spectrometer. By the atmospheric transmissometer, we can calculate the atmospheric transmittance accurately, which can be employed to correct and determine the boundary value of the Lidar effectively. Meanwhile, because the atmospheric transmissometer and particle size spectrometer can measure atmospheric optical properties near the ground, the issue of incomplete overlap zone can be settled to a certain extent. Moreover, in most airports, the atmospheric transmissometer is necessary, and Lidar, as an effective tool of windshear detection, is being popularized around the world gradually, thus it is convenient to set up this combined Lidar system for practical application in the future.

II. GUIDELINES FOR MANUSCRIPT PREPARATION

The combined detection system is composed of Lidar, atmospheric transmissometer and particle size spectrometer, as is shown in Fig. 1. The entire system is fixed at the end of the runway of Tianjin airport, and its specific technical parameters are shown in Table I. We use the VAISALA LT31 as the atmospheric transmissometer, because it is the most common model for visibility detection in the airport. With the atmospheric visibility meter, we can calculate the atmospheric transmittance between the transmitting end and the receiving end by detecting the light intensity after the light beam passes through the air column in the baseline. The particle size spectrometer is fixed near the Lidar to detect properties of atmospheric aerosol on the ground. The model is selected to be GRIMM #1.109, which has 31 channels, and can measure the particle size distribution between 0.25 and 32 μm, the mass concentration of PM2.5 and PM10, as well as the relative humidity. By this combined detection system, we can establish the relationship between PM2.5 mass concentration and atmospheric transmittance, and combined with the atmospheric transmittance profile retrieved by Lidar, the vertical distribution of PM2.5 mass concentration can be calculated effectively.

III. METHOD

A. The Relationship Between PM2.5 Mass Concentration and Atmospheric Transmittance

According to the definition of the mass concentration of particulate matter, the concentration of all particulate matter in the atmosphere [8] can be expressed as

$$C_{\mathrm{PM}\infty} = \int_0^\infty \frac{4}{3}\pi\rho r^3 n(r)_{\mathrm{dry}}\mathrm{d}r \tag{1}$$

where r is the particle radius, ρ is the dry aerosol density, and $n(r)_{\mathrm{dry}}$ is the scale spectrum distribution function of the dry aerosol. The mass concentration of PM2.5 can be demonstrated as

$$C_{\mathrm{PM2.5}} = \int_0^{2.5} \frac{4}{3}\pi\rho r^3 n(r)_{\mathrm{dry}}\mathrm{d}r \tag{2}$$

According to Mie scattering theory [30], the extinction coefficient of dry aerosol in the atmosphere is defined as

$$\sigma_{\mathrm{dry}} = \int_0^\infty \pi Q_{\mathrm{ext}} n(r)_{\mathrm{dry}} r^2 \mathrm{d}r \tag{3}$$

where Q_{ext} is the extinction efficiency factor of aerosol particles.

When the relative humidity in the air is high, the particles will absorb moisture and cause the particle radius to expand, which will causes the extinction coefficient to change significantly. In addition, the relative humidity may also enhance the gas-particle conversion in atmosphere. According to the extinction characteristics of dry and wet aerosols, the moisture absorption growth factor [17], [31] is defined as

$$f(\mathrm{RH}) = \frac{\sigma_{\mathrm{RH}}}{\sigma_{\mathrm{dry}}} \tag{4}$$

that is, the ratio of the extinction coefficient of the wet aerosol $\sigma_{\mathrm{RH}}$to the one of the dry aerosol σ_{dry}. It reflects the influence of water vapor on atmospheric extinction.

Combining equations (1)-(4), the relationship between atmospheric extinction coefficient and PM2.5 mass concentration can be obtained as

$$\sigma_{\mathrm{RH}} = \frac{3\overline{Q}_{\mathrm{exy}} f(\mathrm{RH})}{4 r_{\mathrm{eff}} \overline{\rho} k} C_{\mathrm{PM2.5}} \tag{5}$$

where $r_{\mathrm{eff}} = \int_0^\infty r^3 n(r)_{\mathrm{dry}}\mathrm{d}r / \int_0^\infty r^2 n(r)_{\mathrm{dry}}\mathrm{d}r$ is the effective particle radius, $\overline{Q}_{\mathrm{ext}}$ indicates the overall extinction efficiency

factor of aerosol particles, $\overline{\rho}$ is the average aerosol density, and $k = C_{\mathrm{PM2.5}}/C_{\mathrm{PM}\infty}$is the mass concentration ratio.

According to Beer-Lambert law [32], the relationship between atmospheric transmittance and atmospheric extinction coefficient is

$$T = \exp\left[-\int_a^b \sigma(h)\mathrm{d}h\right] \tag{6}$$

that is, in the optical transmission path from point a to point b, the integration of the extinction coefficient to the path. Note that the Beer's law is just an approximation without considering the multiple scattering and emission of atmospheric layers. According to the relationship between the atmospheric extinction coefficient and the mass concentration of particulate matter in equation (5), we can obtain

$$T = \exp\left[-\int_a^b \frac{3\overline{Q}_{\mathrm{ext}} f(\mathrm{RH})}{4r_{\mathrm{eff}}\overline{\rho}k} C_{\mathrm{PM2.5}}(h)\mathrm{d}h\right] \tag{7}$$

Assuming that in the short distance point a to point b, the type of aerosol, the particle size spectrum and the components do not change, the relationship between the concentration of PM2.5 and the atmospheric transmittance can be calculated as

$$C_{\mathrm{PM2.5}} = -K \cdot \ln T / f(\mathrm{RH}) \tag{8}$$

Among them, the proportional coefficient K can be expressed as $K{=}4r_{\mathrm{eff}}\overline{\rho}k/3(b-a)\overline{Q}_{\mathrm{ext}}$, $b-a$ is the minimum resolution distance of the Lidar. When the relative humidity is high, the particles quickly absorb moisture and expand, which will affect the accuracy of the proportional coefficient K and the detected PM2.5 mass concentration. Therefore, for the relative humidity$>40\%$, the calculated proportional coefficient K needs to be corrected. According to the empirical formula obtained from the research of literature [13], when the relative humidity is below 40%, the moisture absorption growth factor $f(\mathrm{RH}) = 1$; when the relative humidity is above 40%, the moisture absorption growth factor $f(\mathrm{RH}) = 1/(1 - \mathrm{RH} + 40\%)$.

According to the reference [4], after the atmospheric aerosol reaches a stable state, due to the mixing effect of turbulence in the lower atmosphere, it can be considered that the spectral distribution and refractive index of the aerosol particles in this area are the same. However, if the relative humidity change at the vertical height is ignored and the relative humidity detected on the ground is regarded as the basis for estimation calculation, the PM2.5 mass concentration profile obtained from the atmospheric transmittance inversion will have errors at high altitudes.

B. Correction of the Vertical Distribution of Atmospheric Transmittance

The power of the backscatter signal at the height z can be expressed by the Lidar equation

$$P(z) = P_0 \frac{\Delta R \cdot A}{z^2} K_{\mathrm{m}} \beta(z) \exp\left(-2\int_0^z \sigma(z)\mathrm{d}z\right) \tag{9}$$

where $P(z)$ is the laser radar echo signal power, P_0 is the laser pulse emission power, ΔR is the range resolution of the laser radar, $\beta(z)$ is the atmospheric backscatter coefficient, A is the area of the telescope, K_{m} is the system constant, and $\sigma(z)$ is the extinction coefficient.

Using Fernald backward integration method to solve the extinction coefficient of the Lidar equation [33], we can obtain where $X(z) = \ln[P(z)z^2]$ is the laser radar echo distance correction signal, S_1 is the aerosol backscatter ratio, $S_2$is the air molecule backscatter ratio, $Z_{\mathrm{c}}$is the boundary value height, $\alpha_1(z_{\mathrm{c}})$ is the extinction coefficient boundary value, and $\alpha_2(z)$ indicates the atmospheric molecular extinction coefficient.

Within the minimum vertical resolution distance of Lidar, it can be considered that the atmosphere is evenly distributed. Therefore, within each minimum resolution distance, the extinction coefficient is converted to atmospheric transmittance according to Beer-Lambert's law, and finally the vertical distribution of atmospheric transmittance can be expressed as

$$T(z) = \exp[-\sigma(z) \cdot L] \tag{11}$$

In this formula, L is the minimum vertical resolution distance of Lidar.

In order to improve the accuracy of Lidar inversion of atmospheric transmittance, atmospheric transmissometer is used to correct the boundary value and vertical distribution of atmospheric transmittance. The specific correction method is shown as follows: select a piece of relatively smooth data at the highest point of the Lidar detection, and calculate the extinction coefficient boundary value and the corresponding atmospheric transmittance boundary value according to equation (6) and the collis slope method [34]. This height is regarded as the calibration point.

Taking the boundary value of the atmospheric transmittance at the calibration point as the center, we expand a certain value in the positive and negative directions to form a temporary boundary value range with a step of 10m, and obtain a number of temporary boundary values of the atmospheric transmittance and the corresponding temporary boundary values of the extinction coefficient.Finally, the temporary boundary value of each extinction coefficient obtained above is substituted into equation (10), shown at the bottom of this page, for calculation, and the vertical distribution of the obtained extinction coefficient is then brought into equation (11) to obtain multiple vertical distributions of atmospheric transmittance and corresponding ground value of atmospheric transmittance.

Taking the location of the atmospheric transmissometer as the reference point, the measured atmospheric transmittance as the reference value, when the ground value of the atmospheric transmittance retrieved by the Lidar and the reference value conform to equation (12), the boundary value and vertical distribution of the atmospheric transmittance are corrected.

$$\frac{|T_{\mathrm{A}} - T_{\mathrm{B}}|}{T_{\mathrm{B}}} = x \tag{12}$$

In the formula,T_{A} is the reference value of atmospheric transmittance, T_{B} is atmospheric transmittance retrieved by Lidar

$$\sigma(z) = -\frac{S_1}{S_2}\alpha_2(z) + \frac{X(z)\exp\left[2\left(\frac{S_1}{S_2}-1\right)\int_z^{z_c}\alpha_2(z)\mathrm{d}z\right]}{\frac{X(z_c)}{\alpha_1(z_c)+(S_1/S_2)\alpha_2(z)} + 2\int_z^{z_c} X(z)\exp\left[2\left(\frac{S_1}{S_2}-1\right)\int_z^{z_c}\alpha_2(z)\mathrm{d}z\right]\mathrm{d}z} \tag{10}$$

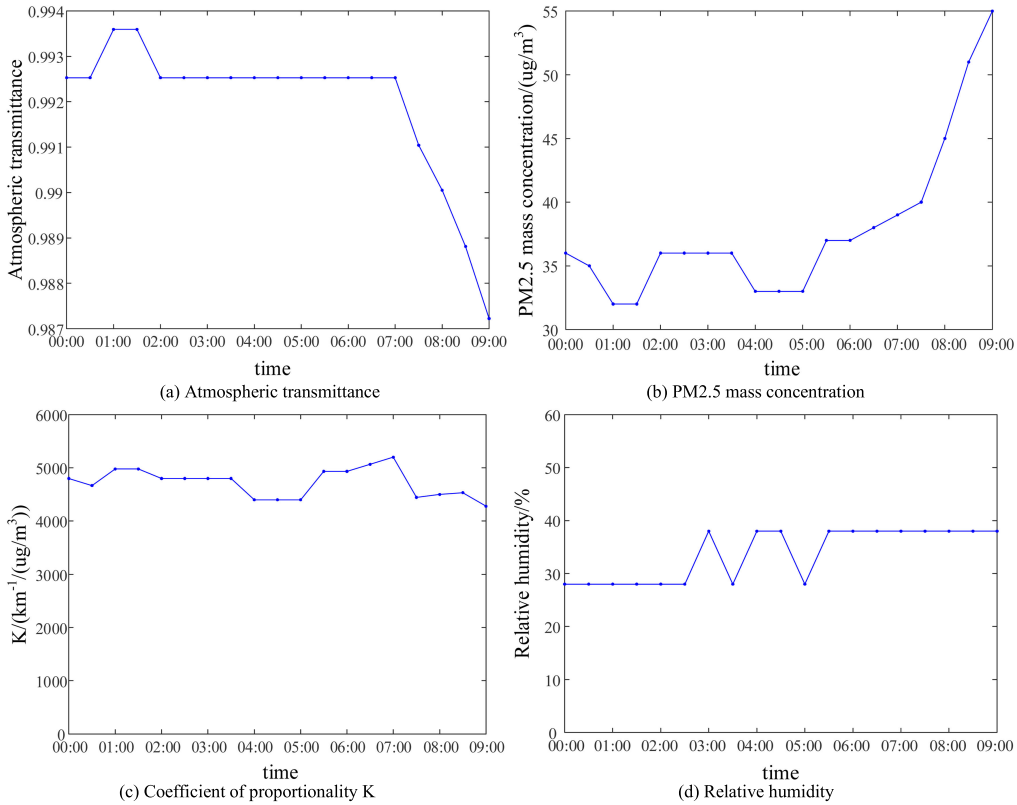

Fig. 2. Changes of parameters with time.

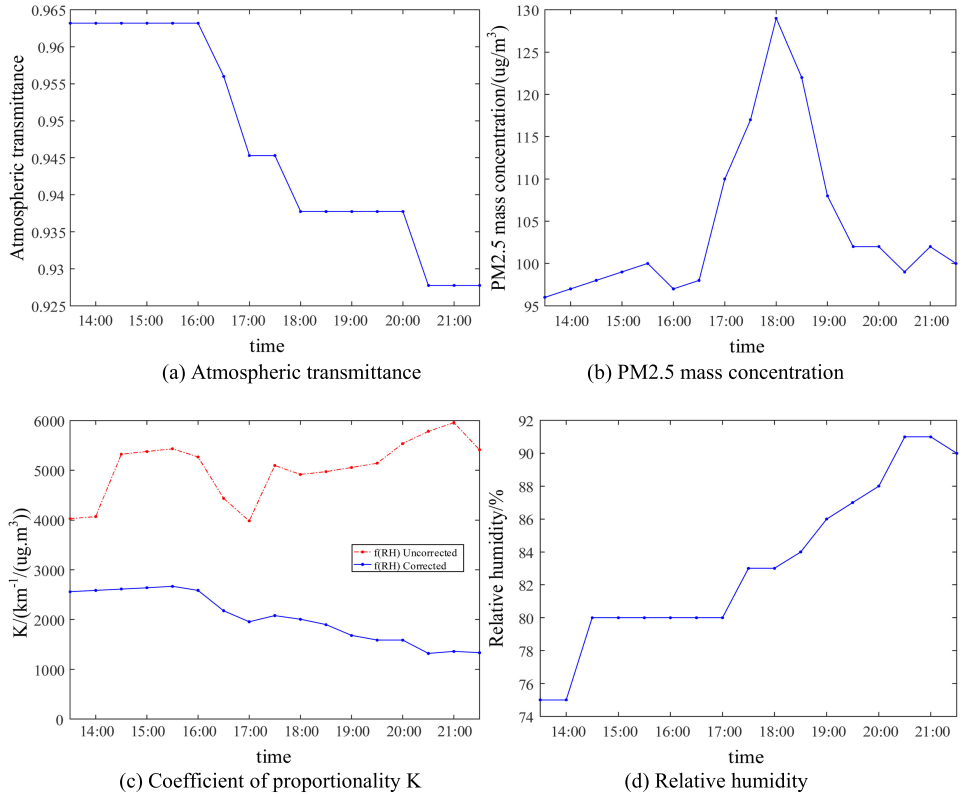

Fig. 3. Changes of parameters with time.

near the ground, and x expresses the adaptive value. According to the given atmospheric transmittance step size, we traverse all its boundary values, and record all the corresponding values $x$at the same time. When the traversal is completed, we select the T_{B} corresponding to the minimum x as the correction value, and the corresponding boundary value as the required boundary value of atmospheric transmittance. This method not only realizes the correction of the boundary value of atmospheric transmittance, but also realizes the correction of the vertical distribution of atmospheric transmittance. According to formula (8), it can be seen that by improving the accuracy of the vertical distribution of atmospheric transmittance, a more accurate PM2.5 mass concentration profile can be calculated. Since this method is based on Fernald backward integration, there will be no cases that the denominator of the Fernald forward integration is zero or negative, which can lead to a infinite or negative inverse value [35].

IV. Experiment and Analysis

A. The Relationship Between Ground PM2.5 Mass Concentration and Atmospheric Transmittance

Using the combined system, we performed the experiments near the airport in Tianjin. According to the deduced negative logarithmic relationship between the atmospheric transmittance and the mass concentration of aerosol particles, we discuss the relationship between ground PM2.5 mass concentration and atmospheric transmittance for different relative humidity ranges. Figs. 2 and 3 show the statistical analysis of atmospheric transmittance, PM2.5 mass concentration and proportional coefficient K in two relative humidity intervals, respectively.

In Fig. 2, we present the atmospheric transmittance, PM2.5 mass concentration as well as the proportional coefficient K varying with the time from 0 to 9 o'clock on December 28, 2017 for the case of low relative humidity. Before 7 o'clock, the atmospheric transmittance remained stable allover, and the PM2.5 mass concentration also fluctuated around the average level. After 7 o'clock, the atmospheric permeability and the mass concentration of PM2.5 began to decline and rise, respectively. However, the proportional coefficient K did not fluctuate seriously. In Fig. 2, it can be seen that the relationship among the scale factor K, atmospheric transmittance, relative humidity and PM2.5 mass concentration conforms to equation (8).

In Fig. 3, for the case of high relative humidity, we demonstrate the atmospheric transmittance, PM2.5 mass concentration as well as the proportional coefficient K varying with the time from 13:30 to 21:00 on December 25, 2017. It can be observed that between 13:30 and 17:00, the relative humidity and PM2.5 mass concentration were in a steady state, thus the atmospheric transmittance remained stable between 13:30 and 16:00; between 17:00 and 18:00, the relative humidity and PM2.5 mass concentration increased rapidly, so the atmospheric transmittance declined. After 18:00, theoretically, as the mass concentration of PM2.5 decreased, the atmospheric transmittance should increase, but due to the effect of relative humidity, the aerosol particles were extremely saturated and extinction

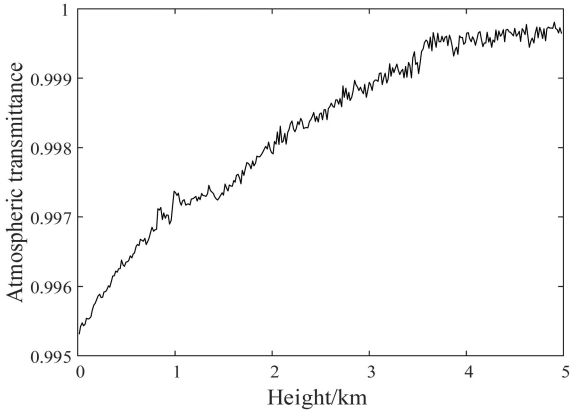

Fig. 4. Vertical distribution of atmospheric transmittance at 12:30 on February 2, 2018.

increased. It can be analyzed from this phenomenon that the decrease in atmospheric transmittance at this time is not caused by aerosol particles, but by water vapor. Therefore, the proportional coefficient K needs to be corrected. Fig. 3(c) shows original and corrected proportional coefficients. It can be observed that the original K fluctuated greatly and did not conform to equation (8), while after correction, the change state and value range of the K value were relatively stable. As a whole, it can reflect the influence of aerosol particles and water vapor on the atmospheric transmittance.

Through the above analysis, it can be found that when the relative humidity is less than 40%, the atmospheric transmittance is negatively correlated with the mass concentration of PM2.5, the proportional coefficient K is mainly affected by the mass concentration of PM2.5, and the proportional coefficient is in a balanced state; when the relative humidity is greater than 40%, the influence of water vapor on the atmospheric permeability and the proportional coefficient K value can not be ignored, especially when the aerosol particles are in the high relative humidity stage, the physical process is more complicated. After the aerosol particles have absorbed moisture and reach saturation, they are easily affected by meteorological conditions such as wind speed and pressure, and when the moisture reaches a certain level, deliquescent and sedimentation will occur, and the proportional coefficient K value is very unstable. After the correction of the moisture absorption growth factor, the proportional coefficient K tends to be stable as a whole, and will conforms to equation (8).

B. Correction of the Vertical Distribution of Atmospheric Transmittance

In Fig. 4, we shows the vertical distribution of atmospheric aerosol transmittance at 12 o'clock on February 2, 2018. In a mild haze weather, the relative humidity of the day was 22%, and the ground visibility measured was 5km. It can be seen from the figure that the atmospheric transmittance range within the vertical resolution distance was between 0.995∼0.9997, and showed an increasing trend from the bottom to the upper air with volatility, especially in the altitude zone of 1-2.5km. On the whole, the vertical distribution of atmospheric transmittance

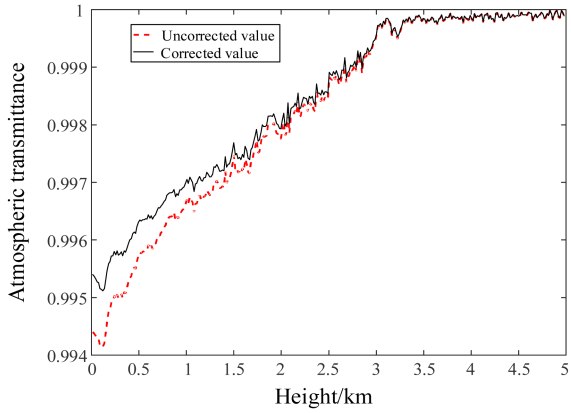

Fig. 5. Comparison of vertical distribution of atmospheric transmittance at 15 in February 10, 2018.

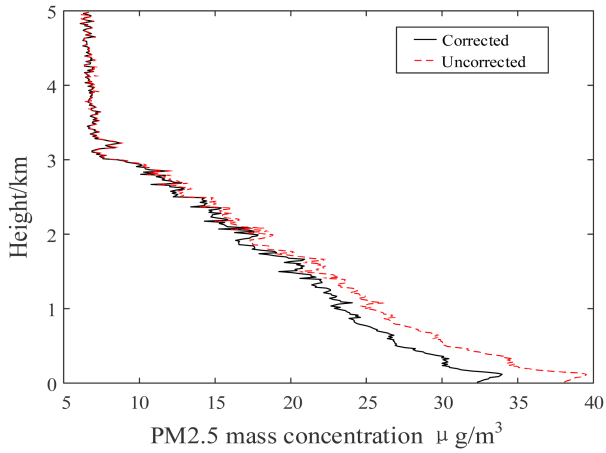

Fig. 6. Comparison of vertical distribution of PM2.5 mass concentration at 15 in February 10, 2018.

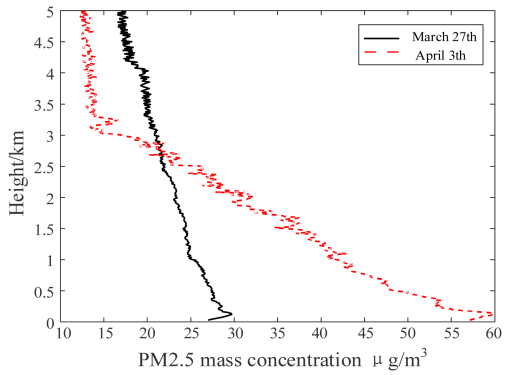

Fig. 7. Vertical inversion of PM2.5 mass concentration.

not only characterizes the optical properties of aerosols at different heights, but also reflects the detailed characteristics of the vertical distribution of aerosols. Note that the data in the overlap zone of Lidar is calculated based on the detection in high-altitude atmosphere, not the result of direct detection.

Fig. 5 shows the comparison of the original and corrected vertical distributions of atmospheric transmittance at 15:00 on February 10, 2018. To evaluate the accuracy of the results, we use the atmospheric transmittance released by Tianjin airport as the standard data. With the proposed method, the visibility on the day was 3.5km, the ground atmospheric transmittance was 0.9955 that is very close to the actual value of 0.9953 in Tianjin airport. It can be observed that there is not much difference between the two curves above 3km height, but below 3km height, the deviation became larger and larger as the height decreases. Under the initial atmospheric transmittance boundary value of 0.9992, the ground value of atmospheric transmittance retrieved by Lidar was 0.9944, which was quite different from the actual value of 0.9953 in Tianjin airport, and greatly affected the vertical distribution error of atmospheric transmittance. After the atmospheric transmittance was corrected by the ground atmospheric transmittance, the corresponding boundary was 0.9994 that is more accurate than the initial boundary of 0.9992. It illustrates that the atmospheric transmittance detected by the atmospheric transmissometer is the main source of uncertainty for our method.

C. PM2.5 Mass Concentration Profile

Fig. 6 shows the comparison of original and corrected spatial distribution of PM2.5 mass concentration at 15:00 on February 10, 2018. To evaluate the accuracy of the results, we employ the PM2.5 released by Tianjin airport as the standard data. After the proportional coefficient K was calculated and moisture absorption factor was corrected with a large amount of data, the relationship between the mass concentration of PM2.5 and the atmospheric transmittance can be expressed as:

$$C_{\mathrm{PM2.5}} = -7110 \ln T \tag{13}$$

At 15:00 on February 10, the relative humidity was 27%, and the ground PM2.5 mass concentration was 32 μg/m^3 in Tianjin airport. In Fig. 6, it can be observed that with the original and corrected vertical distribution of atmospheric transmittance, the PM2.5 mass concentration of 38μg/m^3 and 32.3 μg/m^{3}at the ground were obtained, respectively. After correction, the PM2.5 mass concentration at the ground is very close to the actual data in Tianjin airport, and the inversion of PM2.5 mass concentration is effectively optimized. It illustrates that the PM2.5 mass concentration detected by the particle size spectrometer is the main source of uncertainty for the proposed method.

Fig. 7 shows the spatial distribution of PM2.5 mass concentration at 16:00 on March 27 and at 11:00 on April 3, 2018. After the proportional coefficient K was calculated and moisture absorption factor was corrected, the relationship between the PM2.5 mass concentration and atmospheric transmittance during detection can be expressed respectively as:

$$C_{\mathrm{PM2.5\_1}} = -4800 \ln T \tag{14}$$

$$C_{\mathrm{PM2.5\_2}} = -3109 \ln T \tag{15}$$

At 16:00 on March 27, the relative humidity was 21%, and the mass concentration of PM2.5 at the ground was 27μg/m^3, and increased to 30 at a height of 0.15km, then at a height of 5km, the mass concentration of PM2.5 gradually decreased. In general, the mass concentration of PM2.5 shows a decreasing trend as the height increases. On April 3, the relative humidity

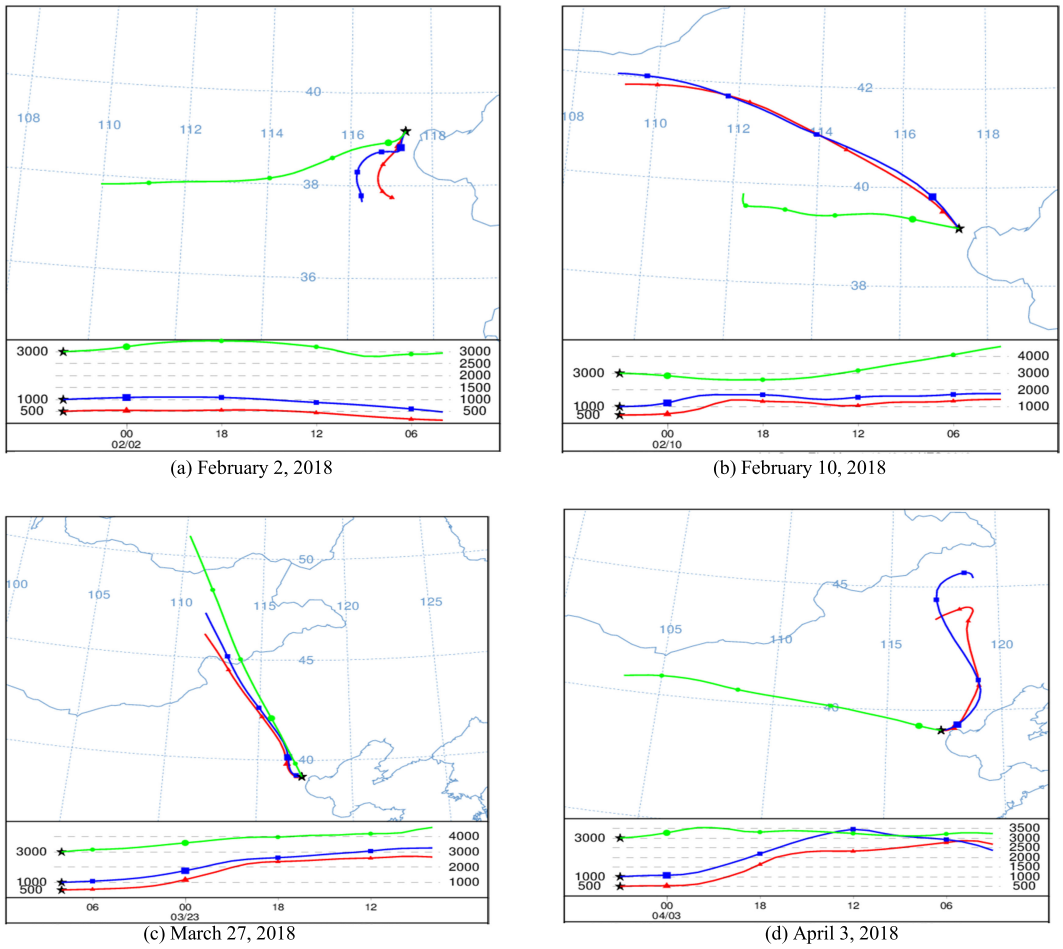

Fig. 8. HYSPLIT backward trajectory.

at 17:00 was 48%, and the mass concentration of PM2.5 on the ground was 52μg/m^3, and still increased to 58 at a height of 0.15km. The mass concentration of PM2.5 in the interval between 0.5 and 2km gradually decreased with the increase in altitude. In the height range of 2$\sim$2.8km, the rate of decrease was greatest, and the mass concentration of PM2.5 was stable above the height of 3km. The vertical distribution of PM2.5 mass concentration at the two detection moments both demonstrate stratification, and the aerosols were mainly concentrated below 3km height. With our method, the detailed characteristics at each level can be fully demonstrated, which reflects microphysical characteristics of the atmospheric aerosols effectively. In general, the two-day PM2.5 mass concentration decreased as the altitude increases, and gradually stabilized after reaching a certain altitude, indicating the typical vertical distribution characteristics of atmospheric aerosols.

D. HYSPLIT Backward Trajectory Analysis

The HYSPLIT model [36] is a professional model of pollutant transport and diffusion developed by the National Oceanic and Atmospheric Administration of the United States. In this paper, the backward trajectory model is used to analyze the transport and diffusion trajectories of aerosol, and then to investigate the effect on the vertical distribution of aerosols [37].

In Fig. 8, we shows the HYSPLIT backward trajectory of above four detections in China. It can be observed that the aerosol distribution at the height of 0.5km and 1km at 12 o'clock on February 2 was caused by the movement of low air masses in Tianjin. The aerosol at a height of 3km was transmitted in parallel from the Shanxi Province. The 0.5km and 1km aerosols at 11 o'clock on February 10 came from a height of 2km in the northwest of Inner Mongolia, while the 3km aerosol came from a 5km high-altitude clean area in the northern part of Shanxi Province, which contained less aerosols, so the mass concentration of aerosols was lower. Fig. 8(c) shows the backward trajectory at 16:00 on March 27. The aerosols at heights of 0.5km and 1km came from the heights of 2.5km and 3km in Mongolia, and the aerosols at heights of 3km came from the height of 4km in the south of Russia, passing through Mongolia and reaching Tianjin. Although the aerosols at the three altitudes have different sources, they are all from the clean air mass of the corresponding altitude. Fig. 8(d) demonstrates the backward trajectory at 11 o'clock on April 3rd. The aerosols at the heights of 0.5km and 1km came from the height of 2.5km in the northeast of China. The trajectory of the air mass at the height of 0.5km was a "J"-shaped path, and the 1km air mass trajectory showed an "S"-shaped path.The aerosol with a height of 3km came from an altitude of 3.5km in the northwest of China. Due to the different

types of aerosols in the two regions, the extinction efficiency of the particles is also different, which might be a possible cause of fluctuations in the aerosol mass concentration distribution at the corresponding time and height in Fig. 6 and Fig. 7.

V. Conclusion

In this paper, we calculated the PM2.5 mass concentration profile based upon the combined detection of Lidar, atmospheric transmissometer and particle size spectrometer. With the combination of transmissive visibility meter and Lidar, the Lidar boundary value can be determined, and the overlap zone of the Lidar can be improved. Compared with the direct use of particle size spectrometer and Lidar to retrieve the PM2.5 mass concentration profile, this method improves the accuracy of the vertical distribution of the intermediate atmospheric transmittance, and optimizes the inversion calculation of the PM2.5 mass concentration profile. Comprehensive research shows that it is feasible to combine Lidar and atmospheric transmissometer to realize the inversion of the vertical distribution of the PM2.5 mass concentration profile. This is of great significance for studying the microphysical properties, scale characteristics of atmospheric aerosols, the transportation and diffusion of aerosols, and providing services for the decision-making of environmental pollution control around the airport.

References

[1] M. Gharibzadeh, K. Alam, Y. Abedini, A. A. Bidokhti, A. Masoumi, and H. Bibi, "Characterization of aerosol optical properties using multiple clustering techniques over Zanjan, Iran, during 2010–2013," *Appl. Opt.*, vol. 57, pp. 2881–2889, 2018.

[2] X. Yang, C. Zhao, L. Zhou, Y. Wang, and X. Liu, "Distinct impact of different types of aerosolson surface solar radiation in China," *J. Geophysical Res. Atmos.*, vol. 121, pp. 6459–6471, 2016.

[3] X. Yang, C. Zhao, L. Zhou, Z. Li, M. Cribb, and S. Yang, "Wintertime cooling and a potential connection with transported aerosols in Hong Kong during recent decades," *Atmospheric Res.*, vol. 211, pp. 52–61, 2018.

[4] R. Caggiano, S. Sabia, and A. Speranza, "Trace elements and human health risks assessment of finer aerosol atmospheric particles (PM1)," *Environ. Sci. Pollut. Res.*, vol. 26, pp. 36423–36433, 2019.

[5] J. Tao, L. M. Zhang, J. J. Cao, and R. J. Zhang, "A review of current knowledge concerning PM2. 5 chemical composition, aerosol optical properties and their relationships across China," *Atmos. Chem. Phys.*, vol. 17, pp. 9485–9518, 2017.

[6] J. Gao, J. Pan, J. Wang, Y. Cai, and Y. Zhao, "Triple charge-coupled device cameras combined backscatter Lidar for retrieving PM2.5 from aerosol extinction coefficient," *Appl. Opt.*, vol. 59, no. 33, 2020, Art. no. 10369.

[7] X. G. Liu, Y. H. Zhang, Y. F. Cheng, M. Hu, and T. T. Han, "Aerosol hygroscopicity and its impact on atmospheric visibility and radiative forcing in Guangzhou during the 2006 PRIDE-PRD campaign," *Atmos. Environ.*, vol. 60, pp. 59–67, 2012.

[8] R. J. Huang *et al.*, "High secondary aerosol contribution to particulate pollution during haze events in China," *Nature*, vol. 514, pp. 218–222, 2014.

[9] X. Ma *et al.*, "Regional atmospheric aerosol pollution detection based on LiDAR remote sensing," *Remote Sens.*, vol. 11, 2019, Art. no. 2339.

[10] H. Ge, W. Gong, J. H. Quan, J. Li, and M. Zhang, "Spatial and temporal distributions of contaminants emitted because of Chinese New Year's Eve celebrations in Wuhan," *Environ. Sci. Proc. Imp.*, vol. 16, pp. 916–923, 2014.

[11] P. F. Liu *et al.*, "Aircraft study of aerosol vertical distributions over Beijing and their optical properties," *Tellus. B.*, vol. 61, no. 5, pp. 756–767, 2009.

[12] A. A. Kokhanovsky, *Aerosol Optics*. Bremen, Germany: Springer, 2008.

[13] S. Wu *et al.*, "Mobile multi-wavelength polarization Raman Lidar for water vapor, cloud and aerosol measurement," *Opt. Exp.*, vol. 23, no. 26, pp. 33870–33892, 2015.

[14] A. Ansmann, M. Riebesell, and C. Weitkamp, "Measurement of atmospheric aerosol extinction profiles with a Raman Lidar," *Opt. Lett.*, vol. 15, no. 13, pp. 746–748, 1990.

[15] H. Xie *et al.*, "Automated detection of cloud and aerosol features with SACOL micro-pulse Lidar in northwest China," *Opt. Exp.*, vol. 25, no. 24, pp. 30732–30753, 2017.

[16] J. Li *et al.*, "Retrieval of aerosol profiles by Raman Lidar with dynamic determination of the Lidar equation reference height," *Atmospheric Environ.*, vol. 199, no. 15, pp. 252–259, 2019.

[17] H. Zhang, Z. Tao, M. Xiaomin, and M. Ma, "Fitting of hygroscopic factor between PM2.5 mass concentration and aerosol backscattering coefficient in Hefei area," *Chin. J. Lasers*, vol. 45, no. 7, pp. 163–169, 2018.

[18] Z. M. Tao, X. M. Ma, and D. Liu, "Statistical distribution of PM2.5 mass concentration profiles at West Suburb of Hefei City in 2014," *Acta Opt. Sin.*, vol. 36, no. 6, pp. 9–17, 2016.

[19] C. Weitkamp, *Lidar Range-Resolved Optical Remote Sensing of the Atmosphere*. New York, NY, USA: Springer, 2005.

[20] S. Grob *et al.*, "Saharan dust contribution to the Caribbean summertime boundary layer – A Lidar study during SALTRACE," *Atmos. Chem. Phys.*, vol. 16, no. 18, pp. 11535–11546, 2016.

[21] T. Nishizawa *et al.*, "Ground-based network observation using Mie–Raman Lidars and multi-wavelength Raman Lidars and algorithm to retrieve distributions of aerosol components," *J. Quant. Spectrosc. Radiat. Transfer*, vol. 188, pp. 79–93, 2017.

[22] K. Meki, K. Yamaguchi, X. Li, Y. Saito, T. D. Kawahara, and A. Nomura, "Range-resolved bistatic imaging Lidar for the measurement of the lower atmosphere," *Opt. Lett.*, vol. 21, pp. 1318–1320, 1996.

[23] J. E. Barnes, N. P. Sharma, and T. B. Kaplan, "Atmospheric aerosol profiling with a bistatic imaging Lidar system," *Appl. Opt.*, vol. 46, pp. 2922–2929, 2007.

[24] J. E. Barnes, S. Bronner, R. Beck, and N. C. Parikh, "Boundary layer scattering measurements with a charge-coupled device camera Lidar," *Appl. Opt.*, vol. 42, pp. 2647–2652, 2003.

[25] E. J. Welton, K. J. Voss, H. R. Gordon, and H. Maring, "Ground-based Lidar measurements of aerosols during ACE-2: Instrument description, results, and comparisons with other ground-based and airborne measurements," *Tellus Ser. B*, vol. 52, pp. 636–651, 2000.

[26] E. J. Welton, J. R. Campbell, J. D. Spinhirne, and V. S. Scott, "Global monitoring of clouds and aerosols using a network of micro-pulse Lidar systems," *Proc. Int. Soc. Opt. Eng.*, vol. 4153, pp. 151–158, 2001.

[27] E. J. Welton and J. R. Campbell, "Micropulse Lidar signals: Uncertainty analysis," *J. Atmos. Ocean. Technol.*, vol. 19, pp. 2089–2094, 2002.

[28] B. N. Chew, J. R. Campbell, J. S. Reid, and D. M. Giles, "Tropical cirrus cloud contamination in sun photometer data," *Atmos. Environ*," vol. 45, pp. 6724–6731, 2011.

[29] B. N. Chew, J. R. Campbell, S. V. Salinas, and C. W. Chang, "Aerosol particle vertical distributions and optical properties over Singapore," *Atmos. Environ.*, vol. 79, pp. 599–613, 2013.

[30] H. C. Hulst and V. Twersky, *Light Scattering by Small Particles*, New York, NY, USA: Dover Publications, 1981.

[31] C. Zhao, Y. Li, F. Zhang, Y. Sun, and P. Wang, "Growth rates of fine aerosol particles at a site near Beijing in June 2013," *Adv. Atmospheric Sci.*, vol. 35, pp. 209–217, 2018.

[32] H. X. Wang, Y. Z. Zhu, and T. Tian, "Characteristics of laser transmission in different types of aerosols," *Acta Phys. Sin.*, vol. 62, no. 2, pp. 324–333, 2013.

[33] Y. Z. Ma, J. Q. Liu, and Q. Q. Wang, "Inversion of aerosol Lidar ratio and its effect on slant visibility based on fernald-PSO method," *Acta Photon.Sin.*, vol. 48, no. 3, 2019, Art. no. 0301001.

[34] R. T. H. Collis and P. B. Russell, "Lidar measurement of particles and gases by elastic backscattering and differential absorption," in *Laser Monitoring of the Atmosphere*, E. D. Hinkley, Ed., Berlin Heidelberg, Germany: Springer, 1976, pp. 71–151.

[35] H. T. Liu, Z. Q. Ge, and Z. Z. Wang, "Extinction coefficient inversion of airborne Lidar detecting in low-altitude by fernald iterative backwark integration method (FIBIM)," *Acta Opt. Sin.*, vol. 28, no. 10, pp. 1837–1843, 2008.

[36] Z. Q. Deng and L. Zhang, "Vertical distributions of dust aerosols derived from CALIPSO and CloudSat observations in Hexi Corridor," in *Proc. IEEE Int. Geosci. Remote Sens. Symp.*, 2016, pp. 4090–4092.

[37] S. Y. Mei, J. J. Ma, and X. Zhang, "Analysis on spatiotemporal variation characteristics of NO_2 concentrations in Beijing-TianJin-Hebei region during APEC," *J. Atmospheric Environ. Opt.*, vol. 11, no. 4, pp. 281–287, 2016.